Available online at www.sciencedirect.com
SCIENCE DIRECT®
International Journal of Heat and Mass Transfer 48 (2005) 3176–3184
International Journal of HEAT and MASS TRANSFER
www.elsevier.com/locate/ijhmt

Spray impingement cooling with single- and multiple-nozzle arrays. Part II: Visualization and empirical models

T.A. Shedd *, A.G. Pautsch

University of Wisconsin-Madison, MFVAL, 1500 Engineering Drive, Madison, WI 53706-1609, USA

Received 1 January 2005; received in revised form 3 February 2005
Available online 20 April 2005

Abstract

The performance of single- and multiple-nozzle sprays for high heat flux electronics cooling using nitrogen-saturated FC-72 was studied in a multi-chip module (MCM) test setup, similar to MCM's used in current high-end computer systems. An additional facility was constructed for visualization of the sprays and heat transfer behavior using clear heating elements coated with an indium tin oxide (ITO) film. Using both the heat transfer and visualization data, it was determined that the heat transfer could be broken down into two or three components: a dominant single-phase component in and around the droplet impact region, a two-phase liquid film boiling component in the corners away from this region, and, for the multiple-nozzle sprays, a single-phase drainage flow component. Empirical models were generated based on this conceptual model, and the correlations predict the data to within about 6%. In addition, a phenomenological critical heat flux (CHF) model was generated based on previous work with thin liquid-film boiling that suggests CHF in thin films occurs due to a homogeneous nucleation mechanism. This model predicts the current data to within about 12% for both single- and four-nozzle arrays.

Keywords: Spay cooling; Heat transfer; Critical heat flux

1. Introduction

The relentless pace of miniaturization of electronics has led to a power-law increase in heat dissipated by common devices. Currently, heat flux densities for microprocessors in desktop computers are near 50 W/cm^2, while processors in some server and supercomputer implementations exceed 75 W/cm^2. By contrast, an electric burner on a consumer kitchen stove generates on the order of 6 W/cm^2. Thus, the heat removal requirements for current and future consumer electronics, as well as high-density laser arrays for communications and military applications, power electronics, and high-power amplifiers for radar systems, are driving the development of effective, compact, and reliable active thermal management systems for high heat flux devices. Spray impingement cooling is growing in prominence and application in the cooling of electronics and laser diodes because spray systems are among the most efficient in terms of heat removed per unit flow rate, and because they may be incorporated into compact packaging at the circuit board level [1]. Significant work has been performed over the past 30 years that has investigated the role of droplet characteristics, liquid film behavior, fluid properties, spray nozzles, flow rates, etc., in spray heat transfer behavior [2–7]. However, a

* Corresponding author. Fax: +1 608 262 8464.
E-mail address: shedd@engr.wisc.edu (T.A. Shedd).

0017-9310/$ - see front matter © 2005 Published by Elsevier Ltd.
doi:10.1016/j.ijheatmasstransfer.2005.02.013

Nomenclature

A	die surface area [cm^2]	ρ	liquid density [kg/m^3]
c_p	liquid specific heat [kJ/kg K]	ave	average across the die
ΔT_{sat}	$T_{sat} - T_{in}$ [K]	in	liquid inlet
h	heat transfer coefficient [W/cm^2 K]	l	liquid
q''	heat flux [W/cm^2]	i	surface
$\overline{Q}$	volumetric flow rate [ml/s]	sat	saturation temperature at local pressure
$\overline{Q''}$	volumetric spray flux [ml/s cm^2]	t	threshold
T	temperature [°C]	j	junction
V	voltage [V]	exp	experimental
ϵ	spray cooling effectiveness [J/ml]	corr	correlation

review of these and other works reveals that few predictive models for heat transfer exist other than for critical heat flux (CHF) [8].

In this study, a prototype of a successful commercial spray impingement cooling system (used in the Cray X1 supercomputer) was used to perform a detailed parametric study of heat transfer performance of single- and four-nozzle spray arrays. The test facility sprays FC-72 onto test chips onto a multi-chip module (MCM) using spray nozzle plates developed by Parker–Hannifin. In addition, a visualization facility with transparent heaters was used to correlate the detailed heat transfer data with local spray and liquid film behavior.

Using these facilities, simple, phenomenological correlations were developed for both single- and multiple-nozzle spray impingement heat transfer that predict the data to within 5% average error. A phenomenological model for critical heat flux (CHF) that predicts the experimental data to within 12% average error was also created. These correlations are based on proposed physical behaviors and appear to allow for the generalization of the predictions beyond the current experiment, as shown by their ability to predict the data for other multiple-nozzle array designs. They also provide a direct indication of the physical nature of the heat removal and CHF mechanisms. For example, these models suggest that phase change plays a minor role in the overall heat removal rate in spray impingement cooling. In addition, the location and surface temperature at which CHF occurs can be determined based on this work for a variety of spray geometries and flow rates.

2. Experimental setup

2.1. Heat transfer measurements

The major features of the test facility and the spray configuration are presented elsewhere [9]. All of the data collected to date are for nitrogen-saturated FC-72, producing a "gas-subcooled" condition, as defined by Horacek et al. [10]. Multiple swirl-atomizing, full-cone spray nozzles were incorporated into a spray plate fabricated by Parker–Hannifin that was positioned 6.8 mm below the test dies such that the sprays were directed upwards onto the heated surface. Heat transfer data were acquired for one spray plate design (referred to as Design 0), shown in Fig. 1, that contained a set of four-nozzle arrays and a set of single nozzles. The test dies were integrated circuits developed and built by IBM Corporation, with eight test dies contained on one MCM, also shown in Fig. 1. Each test die contained four resistive heating elements that could be set to the same power or powered independently to simulate hot and cold regions on the die surface; a uniform heat flux was used for these experiments. Each test die was built with nine solid-state temperature sensors (diodes) integrated into the silicon. Of the eight sensors that were monitored, three were located in the corners of the die, four were located in the center of each of the four quadrants, and one was at the center of the die. The temperatures recorded by the sensors accurately reflected the junction temperature of devices on an integrated circuit; the diode sensors were calibrated to within ±0.2 °C uncertainty in a precision environmental chamber [11].

2.2. Visualization

A second facility was fabricated in which pure ethyl alcohol was circulated by a pump through a spray cap identical to the cap used for heat transfer measurements. In place of the simulated MCM, a clear acrylic substrate with electrically powered glass heaters attached was used. The 17×17 mm square heaters were 0.5 mm thick and made of Corning 1737 aluminosilicate glass, one side of which was coated with indium tin oxide (ITO). Connections were made between

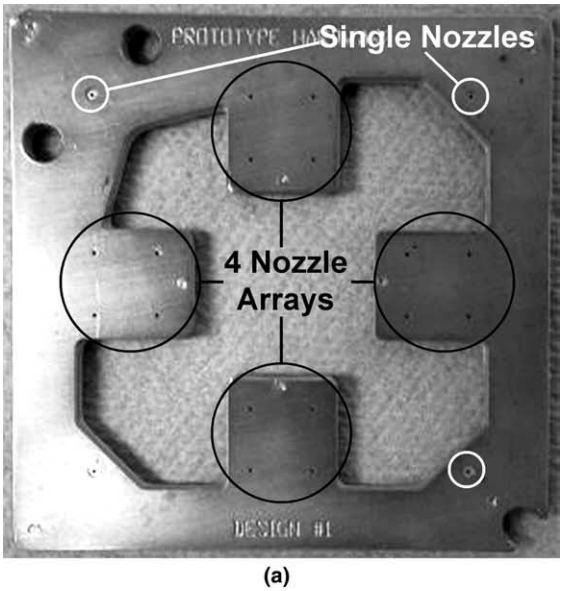

Fig. 1. (a) Spray plate used for heat transfer data. (b) Diagram of multichip module (MCM) with test dies.

copper wires positioned along two sides of a heater and the ITO coating via conductive silver-filled epoxy. The heaters exhibited greater than 95% transparency, allowing for unobstructed observation of the heat transfer processes occurring at the heater surface. The visualization test stand schematic is shown in Fig. 2.

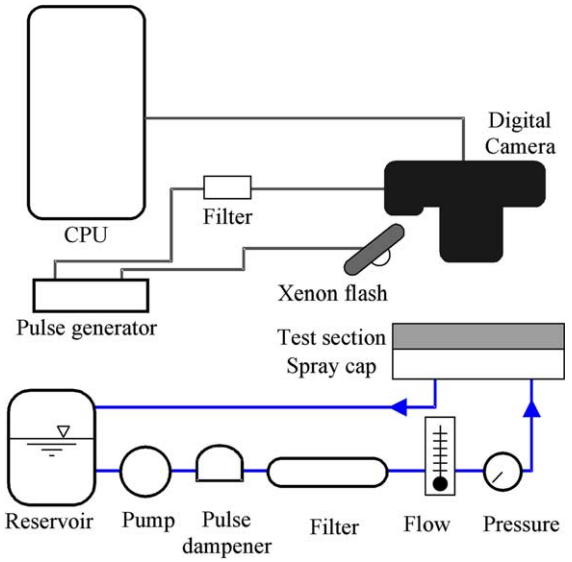

Fig. 2. Schematic of the visualization test stand.

3. Results

3.1. Heat transfer

Fig. 3 presents the overall heat transfer results for the chips cooled by the single- and four-nozzle sprays. The heat transfer coefficient is defined as

$$h = \frac{q''}{T_i - T_{in}}, \tag{1}$$

where T_i is the local die junction temperature and T_{in} is the inlet coolant fluid temperature. The open symbols in Fig. 3 indicate the point at which CHF occurred for each test.

3.2. Temperature variations

Although it has been speculated that spray cooling results in a uniform surface temperature [12], the current data show that large variations in the local surface temperatures existed across the dies. This is shown in Fig. 4 where the maximum temperature variation is plotted at two different conditions, the nominal operating condition of $T_j = 80\ ^\circ C$ and at CHF. These variations are quite significant, reaching as high as 15 and 17 °C at the nominal junction temperature, which could have a significant impact on the performance of large integrated circuits.

3.3. Visualization

As shown in Fig. 4, there is significant variation in the surface temperature across the heater surface

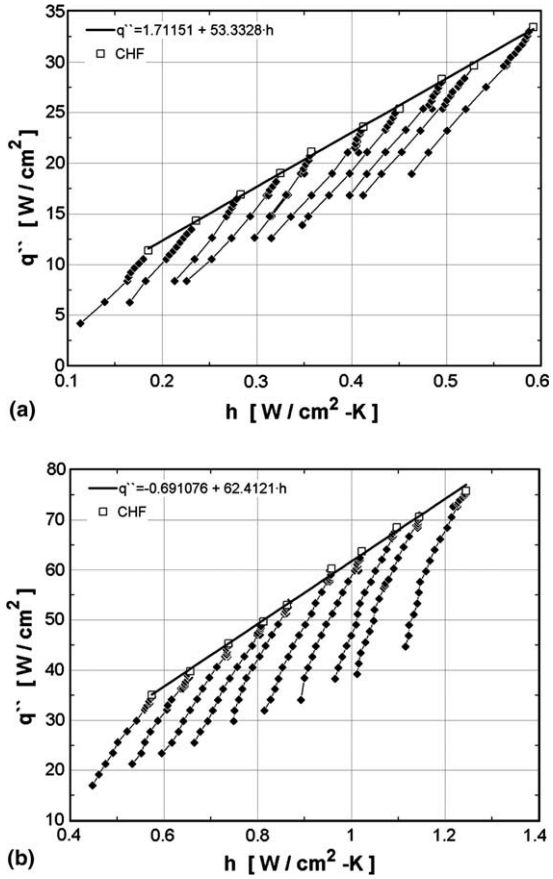

Fig. 3. Heat flux (q'') plotted against heat transfer coefficient (h) for the test chips cooled using single-nozzle sprays (a) and four-nozzle sprays (b). Each data set represents increasing heat flux at a given flow rate where the flow rates spanned the range allowed by the instrumentation (about 0.075–0.25 ml/s per single nozzle, about 0.4–1.2 ml/s per set of four nozzles). The solid line represents the critical heat flux as a function of flow rate.

corresponding to differences in the local heat transfer coefficients across the die. In previous work with these test dies, it was found that the single-nozzle design reached critical heat flux at the corner of the die [9]. This can be explained almost entirely through visualization of the heater surface, samples of which are shown in the top left section of Fig. 5. The droplet flux distribution in the spray visualization correlates fairly well with the heat transfer data in which a peak in heat transfer is found at the center of the die, lower performance is found at the corners, and the lowest heat transfer is found at the quadrant centers. Heat transfer is high where droplets impact the heater with high velocity and frequency, maintaining a thin, well-mixed film of liquid. As the fluid moves away from the center, the film

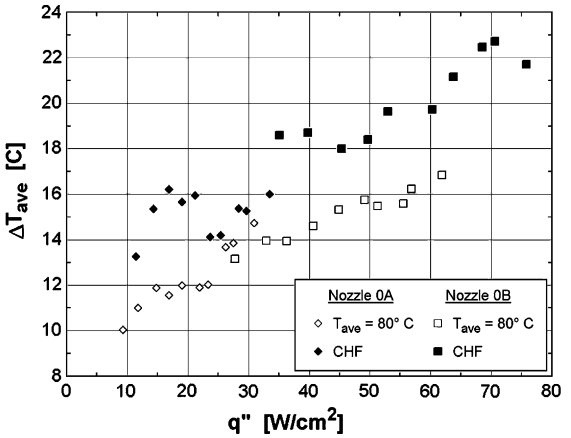

Fig. 4. Average temperature variation across single- and four-nozzle test chips.

becomes thicker and less agitated, and larger ripples are observed in this region. However, a significant portion of the film may not have reached the saturation temperature yet, so nucleate boiling does not appear to take place in this region. Thin film boiling appears to be strongest in the corners where the film moves even more slowly and where it is likely that the bulk of the liquid has reached the saturation temperature. Critical heat flux, or burnout, discussed in detail below, occurs in this region, even though higher heat transfer occurs here compared with the quadrant centers, due to the presence of saturated liquid and vigorous boiling.

In previous studies where the local heat transfer was measured, heat transfer is best at locations of peak droplet flux. However, the four-nozzle spray heaters showed the lowest heat transfer performance at the center where the droplet flux is greatest. Also, critical heat flux always occurred at the center of these heaters. The reason for this behavior becomes apparent from the visualization, shown in the bottom left section of Fig. 5. Fluid from the four sprays impacts the heater surface, spreading outward from the spray cone centers. The liquid film from all four sprays experiences a stagnation point in the center of the die, where virtually all of its initial momentum must be redirected toward one of the four draining paths. Visualization of bubbles using a three-color strobe technique [13] indicated that the fluid motion in this region was very chaotic and that velocities were lower than in the thin film surrounding the sprays. This behavior leads to the thickest films with the slowest moving liquid and lowest heat transfer occurring at the center. Once the applied heat flux reaches a level sufficient to heat the fluid flowing into the center region to saturation, entrained bubbles will grow rapidly, leading to critical heat flux.

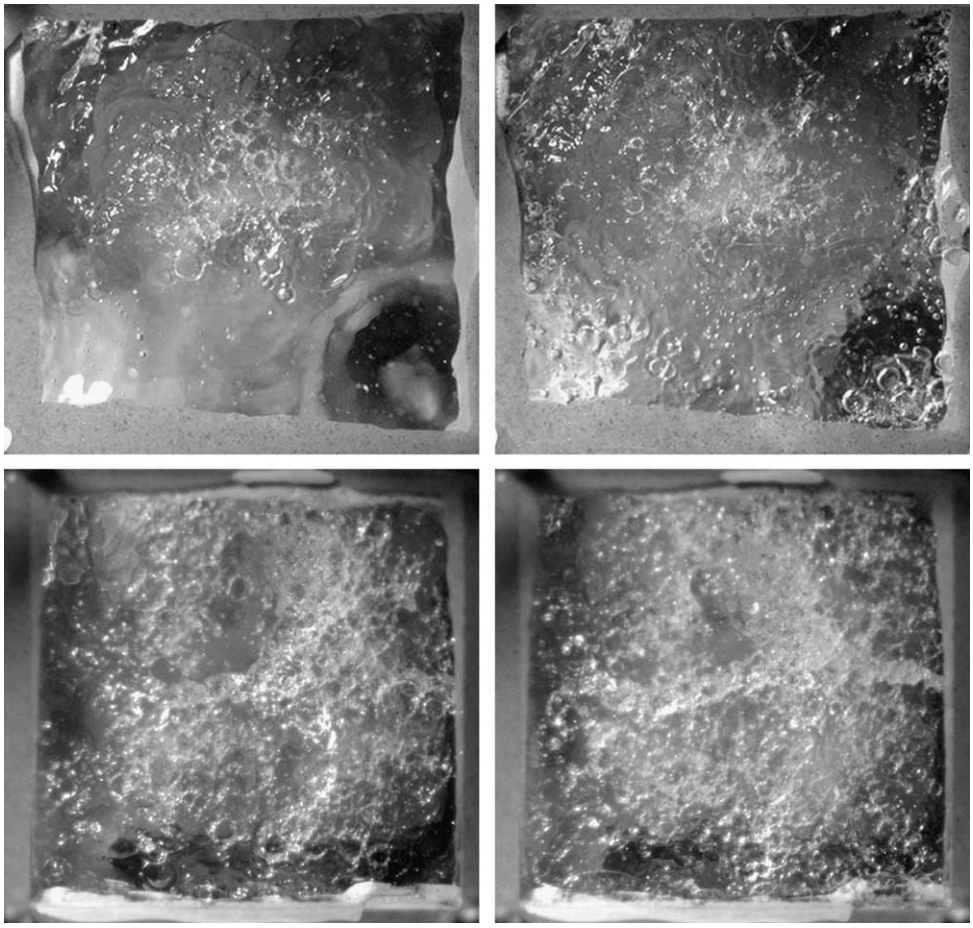

Fig. 5. A visualization of spray nozzles 0A (top) and 0B (bottom). The left picture is the adiabatic case. The right pictures are with applied heat fluxes of 28 W/cm^2 (top) and 18 W/cm^2 (bottom).

4. Empirical models

4.1. Heat transfer

The heat transfer coefficients, plotted in Fig. 3, indicate a strong, nearly linear correlation with flow rate and a weak influence of applied heat flux. These observations, which are consistent with the results of other investigators using many fluids, imply that the heat transfer behavior in spray cooling is dominated by single phase convection, with two-phase evaporation playing a significant, but secondary, role. The top half of Fig. 5 shows images of the heater surface with no applied heat flux (left) and with 25 W/cm^2 applied (right). In both images, the region of droplet impacts is visible at the center of the heater. Without applied heat, the liquid film flowing out from the spray region is generally smooth and thin and carries a number of bubbles. With the applied heat flux, however, nucleate boiling is clearly visible in the thin film. Although the total number of bubbles in the film is not that much greater than in the adiabatic case, it appears that these bubbles, or those originating from nucleation sites on the heater surface, are growing and bursting rather vigorously. Visualization of the four-nozzle sprays had qualitatively similar behavior, though with much less area covered by the smooth film outside of the spray impact region.

The heat transfer data, together with the visualization, led to the development of a model for single- and multiple-nozzle spray cooling heat transfer. Conceptually, the energy transfer modes can be split between single-phase convection and two-phase thin film boiling. The single-nozzle data were fit to a correlation of the form

$$h_{\mathrm{corr,l}} = 0.4627\rho_{\mathrm{l}}c_{p,\mathrm{l}}\overline{Q''} + 0.01612\overline{Q''}\Delta T_{\mathrm{sat}}, \tag{2}$$

where ρ_{l} is the liquid density, $c_{p,\mathrm{l}}$ is the liquid specific heat, $\overline{Q''}$ is the spray volumetric flux, or Q/A, and ΔT_{sat} is the wall superheat above the incoming liquid saturation temperature at the test section pressure. The

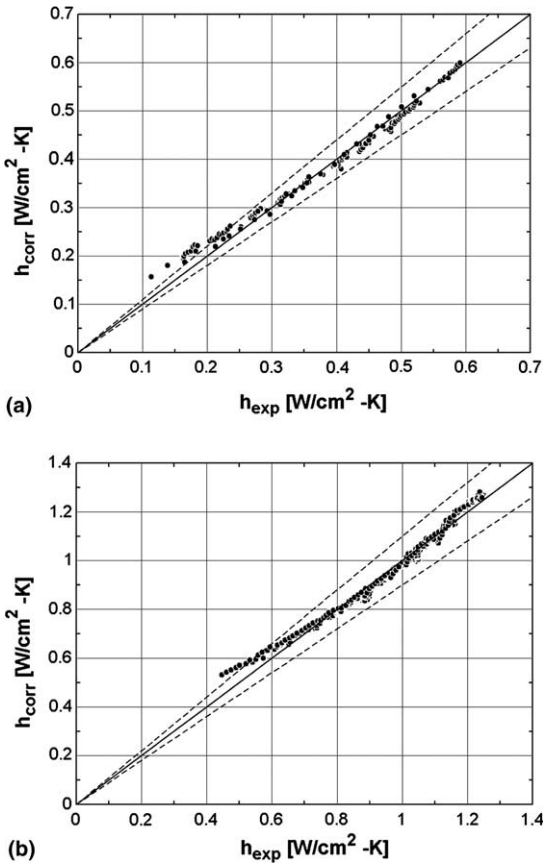

Fig. 6. Plots comparing the predicted heat transfer coefficient with the experimental ones for the single nozzle sprays (a) and the four nozzle sprays (b).

reference area is the total heater area. Eq. (2) correlated the data to within an absolute average error of 5.3%, as shown in the Fig. 6(a). The first term in the correlation represents the single-phase convection contribution, while the second term represents the heat flux dependent contribution, which, based on the visualization experiments, is assumed to characterize thin film boiling.

The first term of Eq. (2) has the dimensions of a heat transfer coefficient (W/cm^2 K). From the visualization experiments, it seems that the constant of the first term represents a ratio of the area in the droplet impact region to the total heater area, but further work is required to verify this. Likewise, further work is needed to physically interpret the second constant in this correlation. However, the nature of the system suggests that it should be related to the spray geometry, liquid properties relating to phase change, and the level of subcooling of the incoming liquid.

It is interesting to note that the boiling term does not depend on ΔT_{sat}^3 as would be expected from pool boiling correlations. However, the linear dependence on ΔT_{sat} is consistent with data for boiling in thin liquid films [14]. On the other hand, this term has a small, but important, volumetric flow component that predicts an increase in two-phase energy transfer mode as the flow rate increases. This is contrary to the predictions offered in the thin film boiling literature where multiple effects (i.e., the increase in nucleation sites as film thickness falls, the increase in conduction through the film, etc.) contribute to increased heat transfer performance as film thickness, or flow rate, decreases [14–17]. This may indicate the effect of bubbles entrained by droplets (secondary nucleation), as the number of entrained bubbles should increase with droplet flow rate.

When the model in the form of Eq. (2) was applied to the four nozzle spray heat transfer data, a good correlation could not be achieved. Flow visualization of the four nozzle sprays, as shown in Fig. 5(b), shows that a cross-like flow pattern develops from the center of the heater to the centers of each side, even at very low flow rates. This led to the hypothesis that an additional term should be added to the heat transfer prediction representing a constant convective term related to the removal of heat by the fluid draining in the cross pattern. It is assumed to be independent of both heat flux and flow rate as a first approximation because the appearance of this drainage flow is relatively unchanged across a wide range of flow and heat flux conditions. With this added term, the four nozzle spray data were correlated to within 2.2% (absolute error) by

$$h_{\mathrm{corr},4} = 0.2284 + 0.2141\rho_l c_{p,l}\overline{Q''} + 0.003812\overline{Q''}\Delta T_{\mathrm{sat}}. \quad (3)$$

The agreement with experimental data is shown in Fig. 6(b). The second and third terms of this equation represent the single- and two-phase energy transfer terms as before, though diminished due to the interference from neighboring sprays.

When data from a total of 10 nozzle designs were added to the analysis, the results were as shown in Fig. 7. Note that the constants in the correlations for single and multiple-nozzle arrays, Eqs. (2) and (3), were not re-optimized for the additional data points. The correlations predict the heat transfer coefficients to within average errors of 6.4% and 9.3% for the single- and multiple-nozzle arrays, respectively.

4.2. Critical heat flux

The cause or causes of CHF in spray evaporative cooling, and thin film boiling in general, are not well known, although Mudawar and Estes have generated a useful model for spray cooling applications [8]. According to Kopchikov et al. [14], high speed films of thin film boiling do not suggest any hydrodynamic limit to the delivery of liquid to the heated surface or to the removal

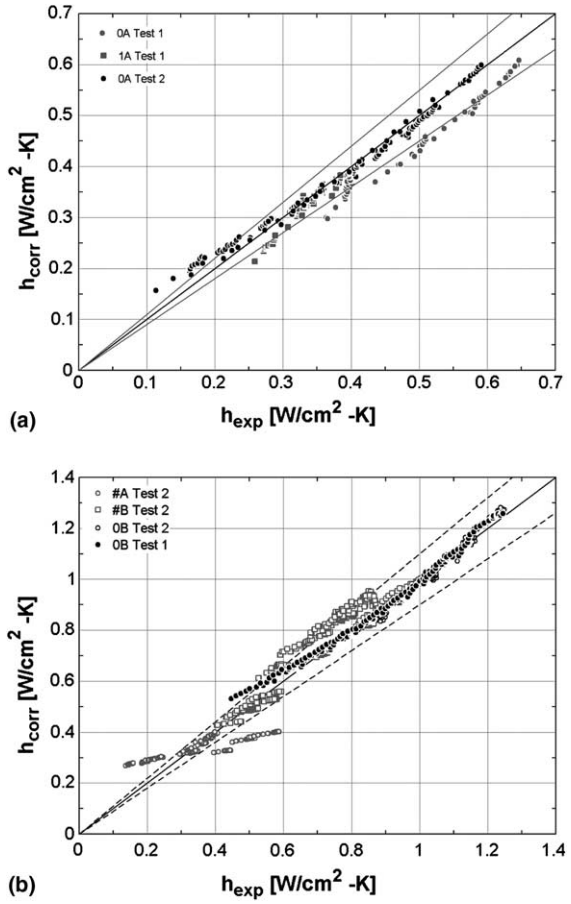

Fig. 7. Heat transfer coefficient predictions for single nozzles (a) and multiple-nozzle arrays (b) using Eqs. (2) and (3), respectively.

of vapor from the liquid interface. They argue that CHF occurs in thin films once the conditions of homogeneous nucleation within the film are reached. Applying this theory to FC-72 predicts a maximum temperature difference between the heated surface and the liquid saturation temperature of 37.0–40.7 °C. CHF data of Estes and Mudawar [18], Mudawar and Deiters [19], and Horacek et al. [10] appear to support this theory, as it predicts reasonably well the maximum temperatures seen in their experiments using different nozzles and liquid subcooling levels. The Kopchikov et al. theory also seems to apply to data for water sprays over a wide range of flow rates obtained by Cui et al. [20], and appears to predict the observations of Mudawar and Valentine [21] for water as well.

The homogeneous nucleation theory was applied directly to both the single- and four-nozzle spray data to predict CHF with good success, as shown in Fig. 8. The prediction is simple:

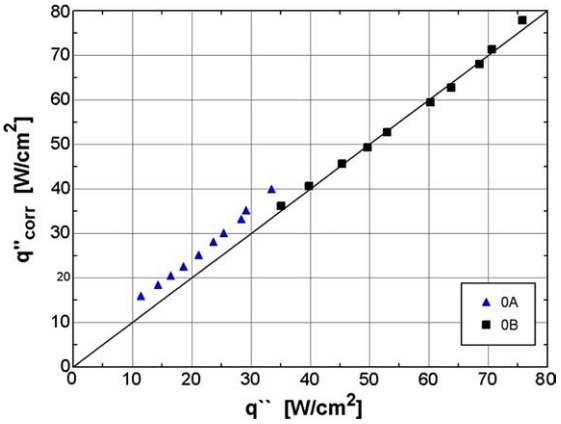

Fig. 8. Comparison of predicted to measured critical heat flux values.

$$\mathrm{CHF} = h\Delta T_{\mathrm{f,crit}}, \tag{4}$$

where h is the heat transfer coefficient predicted by Eqs. (2) or (3) and

$$\Delta T_{\mathrm{f,crit}} = (T_{\mathrm{sat}} + \Delta T_{\mathrm{crit}}) - \left(T_{\mathrm{f}} + \frac{\Delta T_{\mathrm{max,var}}}{2}\right), \tag{5}$$

with ΔT_{crit} calculated as suggested by Kopchikov et al. [14] (37.0–40.7 °C for the conditions of this study) and $\Delta T_{\mathrm{max,var}}$ equal to the maximum temperature variation across the die at CHF. This last term is needed to correct for the fact that the heat transfer coefficient prediction is based on an average die temperature and would overpredict the maximum heat flux based on the peak temperature due to the wide temperature variations noted earlier.

As can be seen in Fig. 8, this model predicts the critical heat flux for the single- and four-nozzle arrays to within 12% on average, though it tends to systematically overpredict the single-nozzle results. Further study is required to explain this behavior.

5. Discussion

5.1. Heat transfer mechanisms

One important theory of spray cooling operation hypothesizes that secondary nucleation, i.e., bubbles entrained by impacting droplets, is a dominant mechanism. Rini et al. [7] performed visualization through a heater with limited transparency (diamond film) and estimated the number, sizes and velocities of bubbles in the liquid film on the heater surface. They suggested that nucleate boiling based on secondary nucleation accounted for 45–50% of the total heat removal rate. Using the models presented above, two-phase mechanisms contribute 25–30% of the total single-nozzle spray cooling heat rate and only 10–20% of the total four-nozzle

spray cooling heat rate. The results of the study to this point do not provide an explanation of the exact nature of this behavior, though it seems closely related to thin film boiling mechanisms [14,22] and mechanisms associated with sliding bubbles [23–26]. In both of these behaviors, vapor generation in bubbles plays only a minor role in the total heat transfer behavior; rather, bubbles serve primarily to mix the liquid layer, enhancing surface evaporation. This agrees with the flow visualization results since large numbers of relatively large bubbles are present in the adiabatic flow images.

For single-nozzle spray impingement cooling, this study found that single-phase heat transfer was dominant and it is possible to hypothesize that with better spray coverage, it may be responsible for 100% of the heat transfer. This is borne out by applying Eq. (2) to the data of Estes and Mudawar [27] who designed their sprays to fill as much of the heater surface as possible. The best fit was obtained by setting the two-phase term to zero and decreasing the single-phase term by a factor of 5. This is in agreement with Estes and Mudawar's assertion that little or no two-phase heat transfer could occur in the small areas left uncovered by the spray.

In the multiple spray nozzle case, a reasonable fit of the data presented by Lin and Ponnappan [28] could be obtained using an equation of the form of Eq. (3), as this data exhibits both the drainage flow contribution and the $\overline{Q''}$ effect on the heat transfer coefficient.

5.2. CHF

Estes and Mudawar [8,27] provide a careful, general and very useful analysis of CHF in spray cooling applications. In generating their correlations, they did not find it necessary to identify the specific mechanisms that cause CHF, but they began their analysis by assuming that CHF began at the outer edges of the heater where the spray coverage was sparse. This study has drawn on the literature describing thin film boiling and breakdown to arrive at a theory that CHF occurs in spray cooling due to homogeneous nucleation in the liquid film rather than any mechanism directly related to the spray. This essentially leads to the breakdown of the liquid at a nearly constant surface superheat for a given fluid, regardless of the inlet subcooling. This is consistent with the data of the Mudawar group, Lin and Ponnappan [28], Cui et al. [20] and Horacek et al. [10]. Some of the water data do not follow this behavior exactly; this may be explained by the stronger heterogeneous nucleation behavior in these films.

6. Summary

In this study, detailed heat transfer and visualization data for single- and four-nozzle array spray cooling was used to develop a better understanding of heat removal mechanisms. Important findings include:

- Single-nozzle spray cooling could be modeled using a superposition of two heat removal mechanisms, single-phase convection in the droplet impact zone and thin-film boiling outside of this region.
- Multiple-nozzle spray cooling could be modeled similarly, with the addition of a constant term representing the effect of constrained drainage flows between spray cones.
- A phenomenological model for critical heat flux was developed that accurately predicts the current spray cooling data.
- These models indicate that in spray cooling systems where a thin liquid film exists on the heated surface, heat removal is dominated by single-phase energy transfer rather than phase-change mechanisms.

Acknowledgement

The authors appreciate the financial support of the University of Wisconsin under the I&EDR funding program, Robert Bolz, and Cray, Inc. Contributions of spray characterization from Parker Hannifin Corp. are also appreciated. The authors thank Natalie Meagher for gathering data and Prof. Greg Nellis for many helpful comments and discussions.

References

[1] G. Pautsch, An overview on the system packaging of the CRAY SV2 supercomputer, in: Proceedings of IPACK'01, The Pacific Rim/ASME International Electronic Packaging Technical Conference and Exhibition, ASME, 2001, pp. 617–624.
[2] S. Toda, A study of mist cooling (1st report: investigation of mist cooling), Heat Transfer: Japanese Res. 1 (1972) 39–50.
[3] L.C. Chow, M.S. Sehmbey, M.R. Pais, High heat flux cooling, Ann. Rev. Heat Transfer 8 (1997) 291–318.
[4] L. Ortiz, J.E. González, Experiments on steady-state high heat fluxes using spray cooling, Experimental Heat Transfer 12 (1999) 215–233.
[5] I. Mudawar, Assessment of high-heat-flux thermal management schemes, IEEE Trans. Compon. Packag. Technol. 24 (2) (2001) 122–141.
[6] J. Li, Spray evaporative cooling in high heat flux electronics, Master's thesis, University of Minnesota, August 2000.
[7] D.P. Rini, R.-H. Chen, L.C. Chow, Bubble behavior and nucleate boiling heat transfer in saturated FC-72 spray cooling, J. Heat Transfer 124 (2002) 63–72.
[8] I. Mudawar, K.A. Estes, Optimizing and predicting CHF in spray cooling of a square surface, J. Heat Transfer 118 (1996) 672–679.

[9] A.G. Pautsch, T.A. Shedd, Spray impingement cooling with single- and multiple-nozzle arrays Part I: Heat transfer data using FC-72, Int. J. Heat Mass Transfer, in press, doi:10.1016/j.ijheatmasstransfer.2005.02.012.
[10] B. Horacek, J. Kim, K.T. Kiger, Effects of noncondensable gas and subcooling on the spray cooling of an isothermal surface, in: Proceedings of the ASME IMECE 2003, American Society of Mechanical Engineers, Washington, DC, 2003, Paper IMECE2003-41680.
[11] A.G. Pautsch, Heat transfer and film thickness characteristics of spray cooling with phase change, Master's thesis, University of Wisconsin-Madison, Madison, Wisconsin, 2004.
[12] M.S. Sehembey, L.C. Chow, M.R. Pais, T. Mahefkey, High heat flux spray cooling: a review, in: A.M. Khounsary, T.W. Simon, R.D. Boyd, A.J. Ghajar (Eds.), Heat Transfer in High Heat Flux Systems, Vol. HTD-Vol. 301 of 1994 ASME International Mechanical Engineering Congress and Exposition, Chicago, IL, 1994, pp. 39–46.
[13] T.A. Shedd, Single- and three-color strobe techniques for bubble/droplet sizing and velocimetry, in: C.-F. Lee (Ed.), ILASS 2002, ILASS Americas, Madison, WI, 2002, pp. 376–380.
[14] I. Kopchikov, G. Voronin, T. Kolach, D. Labuntsov, P. Lebedev, Liquid boiling in a thin film, Int. J. Heat Mass Transfer 12 (1969) 791–796.
[15] P.J. Marto, D.K. MacKenzie, A.D. Rivers, Nucleate boiling in thin liquid films, in: J.W. Palen, R.P. Stein, R.W. Lyczkowski (Eds.), Nuclear, Solar and Process Heat Transfer, Vol. 73–164 of AIChE Symposium Series, St. Louis, MO, 1977, pp. 228–235.
[16] T. Fujita, T. Ueda, Heat transfer to falling liquid films and film breakdown—I: Subcooled liquid films, Int. J. Heat Mass Transfer 21 (1978) 97–107.
[17] V.I. Tolubinskiy, V.A. Antonenko, Y.N. Ostrovskiy, Heat transfer during vaporization in thin films, Heat Transfer—Soviet Res. 14 (6) (1982) 109–114.
[18] K.A. Estes, I. Mudawar, Comparison of two-phase electronic cooling using free jets and sprays, Trans. ASME—J. Electron. Packag. 117 (1995) 323–332.
[19] I. Mudawar, T.A. Deiters, A universal approach to predicting temperature response of metallic parts to spray quenching, Int. J. Heat Mass Transfer 37 (3) (1994) 347–362.
[20] Q. Cui, S. Chandra, S. McCahan, The effect of dissolving salts in water sprays used for quenching a hot surface: Part 2. Spray cooling, J. Heat Transfer 125 (2) (2003) 333–338.
[21] I. Mudawar, W.S. Valentine, Determination of the local quench curve for spray-cooled metallic surfaces, J. Heat Treatment 7 (1989) 107–121.
[22] R. Mesler, G. Mailen, Nucleate boiling in thin liquid films, AIChE J. 23 (6) (1977) 954–957.
[23] G.E. Thorncroft, J.F. Klausner, The influence of vapor bubble sliding on forced convection boiling heat transfer, J. Heat Transfer 121 (1999) 73–79.
[24] B.B. Bayazit, D.K. Hollingsworth, L.C. Witte, Heat transfer enhancement caused by sliding bubbles, J. Heat Transfer 125 (3) (2003) 503–509.
[25] D.B.R. Kenning, O.E. Bustnes, Y. Yan, Heat transfer to a sliding bubble, Multiphase Sci. Technol. 14 (1) (2002) 75–94.
[26] S.D. Houston, K. Cornwell, Heat transfer to sliding bubbles on a tube under evaporating and non-evaporating conditions, Int. J. Heat Mass Transfer 39 (1) (1996) 211–214.
[27] K.A. Estes, I. Mudawar, Correlation of Sauter mean diameter and critical heat flux for spray cooling of small surfaces, Int. J. Heat Mass Transfer 38 (16) (1995) 2985–2996.
[28] L. Lin, R. Ponnappan, Heat transfer characteristics of spray cooling in a closed loop, Int. J. Heat Mass Transfer 46 (20) (2003) 3737–3746.